arXiv:cond-mat/0204013v1 [cond-mat.supr-con] 1 Apr 2002

Two-gap superconductivity in MgB_2: clean or dirty?

I. I. Mazin,[1] O. K. Andersen,[2] O. Jepsen,[2] O. V. Dolgov,[2] J. Kortus,[2] A. A. Golubov,[3] A. B. Kuz'menko,[4] and D. van der Marel[4]

[1] *Center for Computational Materials Science, Naval Research Laboratory, Washington, DC 20375-5000, USA*
[2] *Max-Planck-Institut für Festkörperforschung, Heisenbergstr. 1, D-70569 Stuttgart, Germany*
[3] *University of Twente, Department of Applied Physics, NL-7500 AE Enschede, The Netherlands*
[4] *University of Groningen, Nijenborgh 4, 9747 AG Groningen, The Netherlands*

(Dated: December 30, 2021)

A large number of experimental facts and theoretical arguments favor a two-gap model for superconductivity in MgB_2. However, this model predicts strong suppression of the critical temperature by interband impurity scattering and, presumably, a strong correlation between the critical temperature and the residual resistivity. No such correlation has been observed. We argue that this fact can be understood if the band disparity of the electronic structure is taken into account, not only in the superconducting state, but also in normal transport.

Most researchers ascribe the superconductivity in MgB_2 [1] to the electron-phonon mechanism, enhanced by interband anisotropy of the order parameter [2, 3]. Interband anisotropy, as expressed by the two-gap model [2, 4], offers a simple explanation of many anomalous experimental findings, most importantly of tunneling and thermodynamic measurements [5]. But there is a strong argument against it: As illustrated in Fig. 1, existing bulk samples of MgB_2 have essentially the *same* critical temperature although their residual resistivities, ρ_0, vary greatly, between 0.4 and 40 $\mu\Omega$ cm. Such a behavior is expected for *s*-wave pairing (Anderson's theorem), but not when *two* gaps are present. In that case one expects T_c to fall with increasing ρ_0. Indeed, impurity interband scattering (magnetic and nonmagnetic) with rate γ_{inter} suppresses two-band superconductivity as: $\Delta T_c \propto \gamma_{\text{inter}}/(\pi T_c)$ [6], and it is tempting to assume that $\gamma_{\text{intra}} \sim \gamma_{\text{inter}} \propto \rho_0$. For a sample with $\rho_0 \sim 40$ $\mu\Omega$ cm it seems unlikely that γ_{inter} can be smaller than πT_c. In fact, the body of experimental evidence (Fig. 1) can be reconciled with the two-gap model only if $\gamma_{\text{inter}} \ll \gamma_{\text{intra}}$. Until this paradox is resolved, the two-gap model for superconductivity in MgB_2 cannot be accepted, despite much compelling evidence. Two further problems are: (a) The high-temperature slope of the resistivity is clearly correlated with the residual resistivity (violation of Matthiessen's rule) [5], and (b) the plasma frequency estimated from the measured infrared reflectivity is 5 times smaller than the calculated one [7, 8, 9].

In this letter we shall show that the paradox can be resolved to support the two-gap model. It turns out that due to the particular electronic structure of MgB_2, the impurity scattering *between* the σ- and π-bands is exceptionally small. Thus, the large variation of the residual resistivities reflects primarily a large variation of the scattering rate *inside* the σ- and the π-bands, while the interband $\sigma\pi$-scattering plays *no* role in normal transport. In the superconducting state, the two different gaps in the σ- and the π-bands are preserved even in dirty samples due to the extreme weakness of the $\sigma\pi$-interband impurity scattering.

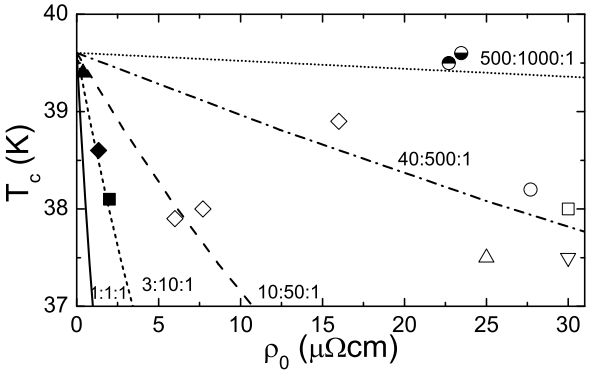


FIG. 1: Critical temperature for samples of varying quality as a function of the residual resistivity. The theoretical curves are computed in the two-band model, according to Ref.[6], with different ratios: $\Gamma_{\sigma\sigma}/N_\sigma(0)$: $\Gamma_{\pi\pi}/N_\pi(0)$: $\Gamma_{\sigma\pi}/N_\pi(0)$. Filled symbols refer to 'high-quality samples': dense wires (▲)[10] and single crystals (◆,■) [11, 12]. Half-filled symbols refer to 'high-T_c, high-ρ' samples [7, 8]. Open symbols refer to samples of intermediate quality (◇, ○, △, ▽, □) [13].

MgB_2 has two π and three σ-bands (Fig. 2) formed by, respectively, the two B p_z and the three bond-orbitals per cell, or, more correctly, by the corresponding Wannier-like functions. A bond orbital is the bonding linear combination of the two B sp^2-hybrids which are directed along a B-B bond. The attractive potential from the Mg^{2+} ions in the hollows between the hexagonal boron layers is felt much stronger by a p_z-electron than by a bond-electron and, as a result, the π-band is pulled so far down in energy that ∼0.17 holes are left at the top of the σ-band. The strong coupling of these holes to the optical bond-stretching modes [14] is what drives the superconductivity. Since the top of the σ-band is at $\mathbf{k}_{\shortparallel} \equiv (k_x, k_y) = \mathbf{0}$ and is doubly degenerate, the holes are distributed in an upper *heavy* and a lower *light* band.

The basic reason why $\sigma\pi$-impurity scattering is small

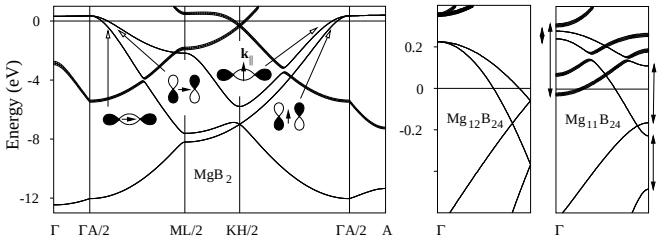


FIG. 2: LMTO bandstructure of MgB_2 along the ΓA-line and in the plane $\left(k_z{=}\frac{\pi}{2c}\right)$ between the ΓMK and ALH-planes, where the σ and π bands (fat) hybridize most. The ΓM/AL-direction is along, and the ΓK/AH-direction is perpendicular to a B-B bond. The orbital characters of the heavy and light σ-bands are explained in the text. $6\times2\times1$ supercell bands for $Mg_{12}B_{24}$ and $Mg_{11}B_{24}$ are shown along the main folding-direction, ΓM. For $Mg_{11}B_{24}$, two extra electrons and protrone dded, and the nuclear charge of each Mg increased by 2/11, to preserve the band filling and electroneutrality.

is that the σ and π-bands are formed from different local orbitals, and therefore are orthogonal on the *atomic* scale, rather than merely on an intermediate scale because of Bloch factors. Moreover, the layered structure and the compactness of the B $2s$ and $2p$ orbitals makes the $\sigma\pi$-disparity in MgB_2 much stronger than, say, the *sd*-disparity in a transition metal, where the *sd*-hybridization gap is almost as large as the *d*-bandwidth.

Specifically, since a p_z-orbital has odd-parity, and a bond-orbital has even parity with respect to the B-layer, the only route for $\sigma\pi$-hybridization is via interlayer hopping, from a p_z-orbital in one layer to a bond orbital in another layer. The corresponding hopping integral, t_{bz}, is, essentially, the geometrical average of the integrals $t_{bb}^{\perp}\sim0.1$ eV and $t_{zz}^{\perp}\sim1$ eV, responsible for the k_z-dispersions of the σ and π-bands [14], and therefore small. Two further factors limit $\sigma\pi$-coupling: The second is that, in its interaction with the nearest bond-orbitals in the next layer, the B p_z-orbital picks up merely the *axial* projection, which is essentially the *s-character*, on the boron above (or below) it. Near the top of the σ-band, the linear combinations of the three bond orbitals are, however, such that the contributions from the B *s*-orbitals *cancel,* so that the top of the σ-band is purely B p_x, p_y-like. Hence, the only source of B *s*-character is tails of B *p*-orbitals centered at other sites. It turns out that the wave-functions for the heavy and light holes ($\nu=h,l$) are: $|\sigma_\nu,\mathbf{k}\rangle \propto \sum_{\mathbf{T}}\left[p_\nu\left(\mathbf{r}+\tau-\mathbf{T}\right)-p_\nu\left(\mathbf{r}-\tau-\mathbf{T}\right)\right]e^{i\mathbf{k}\cdot\mathbf{T}}$, where $\mathbf{T}$ are the lattice translations, $\pm\tau$ are the positions of the two borons in the cell (i.e., in a bond), and $p_{h/l}\left(\mathbf{r}\right)$ is a B *p*-orbital directed transverse/longitudinal to the $\mathbf{k}_{\shortparallel}$-vector. From this representation, illustrated in Fig. 2, it may be realized that the B *s*-character often vanishes completely, and that it generally vanishes proportional to $k_{\shortparallel}^2$ for the heavy-holes, and proportional to $k_{\shortparallel}$ for the light holes. The third limiting factor is the matching of the phase, φ, between the two p_z-orbitals in a bond, $|\pi_{\mp},\mathbf{k}\rangle \propto \sum_{\mathbf{T}}\left[p_z\left(\mathbf{r}+\tau-\mathbf{T}\right)e^{i\varphi(\mathbf{k}_{\shortparallel})}\mp p_z\left(\mathbf{r}-\tau-\mathbf{T}\right)\right]e^{i\mathbf{k}\cdot\mathbf{T}}$, and the phase between the corresponding B *s*-characters arising from the antibonding combination, $p_n\left(\mathbf{r}+\tau\right)-p_n\left(\mathbf{r}-\tau\right)$. In the nearest-neighbor orthogonal tight-binding model for the π-bands, $\varphi\left(\mathbf{k}_{\shortparallel}\right)=\arg\left\{1+e^{i\mathbf{k}\cdot\mathbf{a}}+e^{i\mathbf{k}\cdot(\mathbf{a}-\mathbf{b})}\right\}$, where $\mathbf{a}$ and $\mathbf{b}$ are the primitive translations of the layer.

Due to their even/odd parity, the σ and π-bands can only hybridize when $k_z\neq\frac{\pi}{c}\times$integer. Even then, as seen in Fig. 2, the π_+-band neither hybridizes with the heavy σ-band when $\mathbf{k}_{\shortparallel}$ is along a bond, nor with the light σ-band when $\mathbf{k}_{\shortparallel}$ is perpendicular to a bond. As may be realized from the pictures of the σ-orbitals (Fig. 2), the crossing with the heavy band occurs because the B *s*-character of that band vanishes exactly along this $\mathbf{k}$-line, and the crossing with the light band occurs because, along that $\mathbf{k}$-line, the B *s*-character is purely antibonding between two borons, whereas the π_+-band is purely bonding ($\varphi=0$). The two $\sigma\pi$-gaps seen in the figure are 0.2–0.3 eV, *i.e.,* the hybridization matrix elements, $|\langle\sigma\mathbf{k}|H|\pi\mathbf{k}\rangle|$, are merely a per cent of the σ and π bandwidths!

We now discuss impurity scattering and use [15]:

$$\Gamma_{nn'}=\frac{2}{\hbar N_n\left(0\right)}\sum_{\mathbf{k}\mathbf{k}'}\delta(\varepsilon_{n\mathbf{k}})|\langle n\mathbf{k}|V|n'\mathbf{k}'\rangle|^2\delta(\varepsilon_{n'\mathbf{k}'}),\quad(1)$$

for the rate of scattering to band n' of an electron in band n, by a weak localized impurity potential, $V\left(\mathbf{r}\right)$. Here, $\sum_{\mathbf{k}}$ denotes the average over the Brillouin zone, $\varepsilon_{n\mathbf{k}}$ is the band energy with respect to the Fermi level, and $N(0)=\sum_n N_n\left(0\right)=\sum_{n\mathbf{k}}\delta(\varepsilon_{n\mathbf{k}})$ is the density of states per spin and cell. Typical defects for MgB_2 are Mg-vacancies and Mg-substitutional impurities, which form easily, and B-site substitutions like N and C, which have a higher energy cost. The potential $V\left(\mathbf{r}\right)$ for a localized Mg-defect has the full point-symmetry of the site and, like the Mg^{2+}potential in the crystal, is felt more by a p_z-orbital than by a bond orbital. Hence, the largest matrix elements are those involving p_z-orbitals near the impurity, i.e., the largest perturbation is of the energies of the p_z-orbitals on the B hexagons immediately above and below the impurity, and of the corresponding $t_{zz}^{\perp}$. This means that $\Gamma_{\pi\pi}$ should be large. Screening perturbs the energies of the bond orbitals surrounding the impurity, and also perturbs $t_{bb}^{\perp}$, but to a lesser extent. Hence, we expect that $\Gamma_{\pi\pi}>\Gamma_{\sigma\sigma}$ for Mg-defects, albeit not for B-site substitutions. What contributes to $\Gamma_{\sigma\pi}$, are matrix elements involving a p_z and a bond-orbital, and most importantly, those on either side of a Mg-defect. Since this matrix element is the perturbation of t_{zb}, it is expected to be intermediate between those of $t_{zz}^{\perp}$ and $t_{bb}^{\perp}$, like for the $\sigma\pi$-hybridization. Moreover, since the impurity potential is fairly constant around a neighboring

boron, a p_z-orbital still picks up merely the B s-character which vanishes as $k_{||}^2$ for the heavy and as $k_{||}$ for the light holes. This makes $|\langle\sigma\mathbf{k}|V|\pi\mathbf{k}'\rangle|$ minute because k_{Fh} and k_{Fl} are very small. Also the mismatch of phases between the σ and π-functions will tend to reduce $|\langle\sigma\mathbf{k}|V|\pi\mathbf{k}'\rangle|$. Finally, squaring this small matrix element and inserting it in (1), leads to an exceedingly small $\Gamma_{\sigma\pi}$.

To gain quantitative understanding of the disparity between the scattering rates we have performed LMTO supercell calculations for various impurities. Since the induced $\sigma\pi$-gaps, $2|\langle\sigma\mathbf{k}|V|\pi\mathbf{k}'\rangle|$, are sensitive to their position within the σ-band (the B s-factor), we must choose a supercell which provides band-foldings near ε_F. The results shown in Fig. 2 were obtained with a $6\times2\times1$ supercell. The bands labeled $Mg_{12}B_{24}$ are the same as those in the left panel, but folded into the smaller zone. The heavy σ-band now crosses itself closely below ε_F, while the heavy-light and light-light crossings are a bit further down. The π_--band (fat) slightly above the top of the σ-band was originally at ML/2 and has been folded 3 times into Γ. The $Mg_{11}B_{24}$ bands illustrate the effects of a Mg-vacancy: While the three π-bands get split by 0.35 eV, and the heavy and light σ-bands by 0.27 eV (but by 0.04 eV at Γ), the $\sigma\pi$-splitting of the heavy band is merely 0.015 eV and that of the light band is merely 0.030 eV! The squares of these splittings give estimates for the corresponding Γ's. For Mg-vacancies therefore,

$$\Gamma_{\pi\pi} > \Gamma_{\sigma\sigma} \gg \Gamma_{\sigma\pi}. \tag{2}$$

We found very similar results for systems in which the Mg-vacancy was compensated by substitution of B by two C or one N: For $Mg_{15}B_{31}N$, the $\pi\pi$-splitting was 0.4 eV, the $\sigma\sigma$-splitting 0.3 eV, and the $\sigma\pi$-splittings less than 0.03 eV.

Let us now investigate how the relation (2) infuences the transport properties. These depend both on the impurity scattering and on the electron-phonon interaction (EPI). The interband anisotropy should be taken into account both in the impurity scattering (as outlined above), and in the EPI. The latter can be characterized by two sets of four spectral functions each: the standard Eliashberg functions $\alpha^2F_{nn'}(\omega)$, which define the superconducting properties and thermodynamical properties like the electronic specific heat and the de Haas-van Alphen mass renormalizations, and the transport Eliashberg functions $\alpha^2_{\rm tr}F_{nn'}(\omega)$. Of the calculated $\alpha^2F_{nn'}(\omega)$ functions [16] (the details of the calculations are as in Ref. [14]), $\alpha^2F_{\sigma\sigma}(\omega)$ exhibits a large peak at $\omega\approx70$ meV. Defining $\lambda_{nn'} = 2\int\omega^{-1}\alpha^2F_{nn'}(\omega)d\omega$, we obtain the partial EPI constants, shown in Table I, which are similar to those obtained in [2]. In the following we assume that $\Gamma_{\rm inter} = 0$, so the clean limit is appropriate (T_c is independent of the intraband Γ's). The superconducting properties in the clean two-band model have been investigated in detail [3, 16]. Therefore we shall now concentrate on the normal transport.

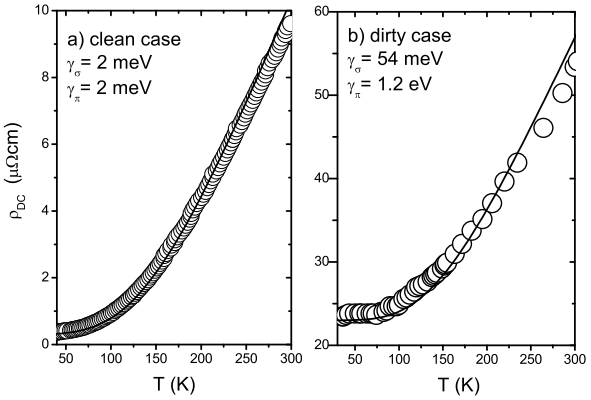


FIG. 3: The DC resistivity in the clean (a) and dirty (b) case compared to experimental data for dense wires [10] and for c-oriented films [7], respectively. The lines are calculated in the effective two-band model with the indicated scattering and *ab initio* plasma frequencies ω_σ^{ab}= 4.14 eV, ω_π^{ab}= 5.89 eV, ω_σ^{c}= 0.68 eV, and ω_π^{c}= 6.85 eV.

The explicit expression for the conductivity in the two-band model is [17] (omitting Cartesian indices)

$$1/\rho_{\rm DC}(T) = \frac{1}{4\pi}\sum_{n=\sigma,\pi}\omega^2_{{\rm pl}\,n}/W_n(0,T)\,, \tag{3}$$

$$W_\sigma(0,T) = \gamma_\sigma + \frac{\pi}{T}\int_0^\infty d\omega\frac{\omega}{\sinh^2(\omega/2T)} \times \left[\alpha^2_{\rm tr}(\omega)F_{\sigma\sigma}(\omega) + \alpha^2_{\rm tr}(\omega)F_{\sigma\pi}(\omega)\right],$$

where $\gamma_\sigma = \gamma_{\sigma\sigma}+\gamma_{\sigma\pi}$, $\gamma_\pi = \gamma_{\pi\pi}+\gamma_{\pi\sigma}$, and $\gamma_{nn'}\simeq2\Gamma_{nn'}$. Eq. (3) is essentially the standard parallel-conductor formula. Our assumptions are that $\gamma_{\pi\sigma}\approx0$ and that γ_σ differs much less than γ_π between 'good' (e.g., Ref.[10]) and 'bad' samples (e.g. [7]).

The role of interband anisotropy, clearly visible in Table I, is different in superconductivity and electric transport. For instance, the critical temperature is given by the maximum eigenvalue of the λ-matrix [15, 17] (*i.e.,* mostly by its maximum element), while the conductivity (3) is the sum of the partial conductivities. At high temperature, therefore, the slope $d\rho/dT$ is determined by $\sum_n\omega^2_{{\rm pl}\,n}/\lambda_{tr\,n}$, *i.e.*, by the smallest $\lambda_{{\rm tr}\,n}\equiv\sum_{n'}\lambda_{{\rm tr}\,nn'}$.

In Fig.3 we show the temperature dependence of the DC resistivity for (a) a clean case with $\gamma_\sigma=\gamma_\pi=2$ meV, and (b) a dirty case with $\gamma_\sigma=54$ meV and $\gamma_\pi=1.2$ eV. In the two cases, all plasma frequencies are the same. The model is seen to describe both cases well. Note that γ_σ and γ_π determine not only the residual resistivity, but also the temperature dependence of the resistivity. In a one-band model, it would be impossible to reconcile the data of Refs. [7, 8] with those of Ref. [10] if they differ only by impurity concentrations, and the corresponding violation of Matthiessen's rule would be totally inexplicable.

Why is the temperature dependence of the resistiv-

	$\lambda_{\sigma\sigma}$	$\lambda_{\pi\pi}$	$\lambda_{\sigma\pi}$	$\lambda_{\pi\sigma}$
transport	0.80	0.41	0.30	0.15
superconducting	1.02	0.45	0.21	0.16

TABLE I: Superconducting and transport coupling constants λ for the effective two-band model. The partial densities of states at the Fermi level for the two bands have values of $N_\sigma(0)$=0.15 and $N_\pi(0)$=0.21 (states/cell· spin·eV).

ity so different in these two cases? Let us compare the clean limit, $\gamma_\sigma = \gamma_\pi = 0$, with the dirty-Mg-layer's limit, $\gamma_\pi = \infty$, $\gamma_\sigma = 0$. Of the two parallel conducting channels, in the former case the π-bands are responsible for conductivity at high temperatures, as was mentioned above, and even at $T \approx 0$ the conductivity is mostly due to the π-bands, their plasma frequency being higher than that one of the σ-bands. Since the EPI constant for the π-bands is small, the temperature dependence of the resistivity is weak. On the contrary, in the dirty case, the π-bands do not conduct, due to an overwhelming impurity scattering, and the electric current is carried only by the σ-bands. It is the strong EPI for this band which causes the temperature dependence of the resistivity in dirty samples..

To conclude, we suggest a new model for electric transport in MgB_2. The main ingredients of the model are (i) *interband* impurity scattering in MgB_2 is small, even in low-quality samples; (ii) *intraband* impurity scattering in the σ-band is small relative to the *intraband* π-band scattering; (iii) high-resistivity samples differ from good samples mostly by the *intraband* π-band scattering rate. Of course, (iv) the phonon scattering is stronger in the σ-band. This model explains well such seemingly inexplicable experimental facts as (1) absence of direct correlation between the residual resistivity and the critical temperature, expected in the two-gap model and (2) a strong correlation between the residual resistivity and the slope $d\rho/dT$ in the normal state. Finally, we would like to point out that the existence of two qualitatively different scattering rates in the two bands should manifest itself in other experiments, such as optical and microwave spectroscopy, or Hall effect. In particular, seemingly mysterious observations of the anomalously small Drude weight in infrared absorption[7, 8, 9] are probably due to overdamping of the Drude contribution from the π-bands, so that the observed Drude peak comes essentially from the σ-bands. The latter have small plasma frequencies and are additionally renormalized by the electron-phonon coupling. At the same time, the overdamped Drude peak from the π-electrons manifest itself as a broad background extending to high frequencies.

JK would like to thank the Schloeßmann Foundation for financial support. IIM acknowledge partial support from the Office of Naval Research.

[1] J. Nagamatsu, N. Nakagawa, T. Muranaka, Y. Zenitani and J. Akimitsu, Nature (London) **410**, 63 (2001).

[2] A. Y. Liu, I. I. Mazin and J. Kortus, Phys. Rev. Lett. **87**, 087005 (2001).

[3] H. J. Choi, D. Roundy, H. Sun, M. L. Cohen, and S. G. Louie, cond-mat/0111182; cond-mat/0111183.

[4] S. V. Shulga, S.-L. Drechsler, H. Eschrig, H. Rosner, and W.E. Pickett, cond-mat/0103154.

[5] C. Buzea and T. Yamashita, Supercond. Sci. Tech. **14**, R115 (2001).

[6] A. A. Golubov and I. I. Mazin, Phys. Rev. B **55**, 15146 (1997).

[7] J. J. Tu, G. L. Carr, V. Perebeinos, C. C. Homes, M. Strongin, P. B. Allen, W. N. Kang, E. M. Choi, H. J. Kim, and Sung-Ik Lee, Phys. Rev. Lett. **87**, 277001 (2001).

[8] A. B. Kuz'menko, F. P. Mena, H. J. A. Molegraaf, D. van der Marel, B. Gorshunov, M. Dressel, I. I. Mazin, J. Kortus, O. V. Dolgov, T. Muranaka, and J. Akimitsu, Solid State Commun. **121,** 479 (2002).

[9] R. A. Kaindl, M.A. Carnahan, J. Orenstein, D.S. Chemla, H.M. Christen, H.Y. Zhai, M. Paranthaman, D.H. Lowndes, Phys. Rev. Lett. **88**, 027003 (2002).

[10] P. C. Canfield, D. K. Finnemore, S. L. Bud'ko, J. E. Ostenson, G. Lapertot, C. E. Cunningham, and C. Petrovic, Phys. Rev. Lett **86**, 2423 (2001).

[11] A. K. Pradhan, Z. X. Shi, M. Tokunaga, T. Tamegai, Y. Takano, K. Togano, H. Kito, and H. Ihara Phys. Rev. B **64**, 212509 (2001); S.Lee, H.Mori, T.Masui, Yu.Eltsev, A.Yamamoto, S.Tajima, J. Phys. Soc. Jpn. **70**, 2255 (2001).

[12] M. Xu, H. Kitazava, Y. Kitazawa, Y. Takano, J.Ye, K.Nishina, H.Abe, A. Matsushita, N. Tsutjii, and G. Kido, Appl. Phys. Lett., **79**, 2779 (2001); A. V. Sologubenko, J. Jun, S. M. Kazakov, J. Karpinski, H.R. Ott, cond-mat/0111273.

[13] M. Dhallé, P. Toulemonde, C. Beneduce, M. Musolino, M. Decroux, and R. Flükiger, Physica C **363**, 155 (2001); B. Lorenz, R. L. Meng, Y. Y. Xue, and C. W. Chu, Phys. Rev. B **64**, 052513 (2001); A. A. Zhukov, A. Purnell, Y. Miyoshi, Y. Bugoslavsky, Z. Lockman, A. Berenov, J. L. MacManus-Driscoll, L. F. Cohen, H. Y. Zhai, H. M. Christen, M. P. Paranthaman, D. H. Lowndes, M. H. Jo, M. G. Blamire, Ling Hao, and J. C. Gallop, cond-mat/0107240; W. N. Kang, C. U. Jung, K. H. P. Kim, M.-S. Park, S. Y. Lee, H.-J. Kim, E.-M. Choi, K. H. Kim, M.-S. Kim, and S.-I. Lee, Appl. Phys. Lett., **79**, 982 (2001); A. Sharoni, O. Millo, G. Leitus, S. Reich, J. Phys.:Cond. Matter **13**, L503 (2001).

[14] Y. Kong, O.V. Dolgov, O. Jepsen, and O.K. Andersen, Phys. Rev. B **64**, 020501 (R) (2001).

[15] P. B. Allen, Phys. Rev. B **13**, 1416, (1976).

[16] A. A. Golubov, J. Kortus, O. V. Dolgov, O. Jepsen, Y. Kong, O. K. Andersen, B. J. Gibson, K. Ahn, and R. K. Kremer, J. Phys.: Cond. Mat. **14**, 1353 (2002); A. Brinkman *et al*, Phys. Rev. B, to be published.

[17] P. B. Allen, Phys. Rev. B **3**, 305 (1971). I. I. Mazin , A. I. Liechtenstein, C. O. Rodriguez, O. Jepsen, and O. K. Andersen, Physica C **209**, 125 (1993).